

Half-soliton interaction of population taxis waves in predator-prey systems with pursuit and evasion

M. A. Tsyganov

Institute of Theoretical and Experimental Biophysics, Pushchino, Moscow Region 142290, Russia

V. N. Biktashev

Department of Mathematical Sciences, University of Liverpool, Liverpool L69 7ZL, United Kingdom

(Received 14 March 2004; published 14 September 2004)

In this paper, we use numerical simulations to demonstrate a half—soliton interaction of waves in a mathematical model of a “prey-predator” system with taxis when of two colliding waves, one annihilates and the other continues to propagate. We show that this effect depends on the “ages” or, equivalently, “widths” of the colliding waves. In two spatial dimensions we demonstrate that the type of interaction, i.e., annihilation, quasisoliton, or half-soliton, depends not only on curvature and width of the colliding waves, but also on the angle of the collision. When conditions of collision are varying in such a way that only a part of a wave survives the collision, then “taxitons,” compact pieces of solitary waves, may form, which can exist for a significant time.

DOI: 10.1103/PhysRevE.70.031901

PACS number(s): 87.10.+e

I. INTRODUCTION

In this paper we continue the study of a system of two spatially distributed populations in a “predator-prey” relationship with each other, started in our previous works [1–3]. The spatial evolution is governed by three processes: positive taxis of predators up the gradient of prey (pursuit) and negative taxis of prey down the gradient of predators (evasion), yielding nonlinear “cross-diffusion” terms, and random motion of both species (diffusion). The resulting mathematical model is a system of two partial differential equations,

$$\begin{aligned}\frac{\partial P}{\partial t} &= f(P, Z) + D\nabla^2 P + h_- \nabla \cdot (P \nabla Z), \\ \frac{\partial Z}{\partial t} &= g(P, Z) + D\nabla^2 Z - h_+ \nabla \cdot (Z \nabla P),\end{aligned}\quad (1)$$

where $P(\mathbf{r}, t)$ is the density of the prey population, $Z(\mathbf{r}, t)$ is the density of the predator population, the nonlinear functions $f(P, Z)$ and $g(P, Z)$ describe local dynamics, including growth and interaction of the species, whereas the diffusion terms describe their spread in space, e.g., resulting from individual random motions. The taxis terms are as in Ref. [4], constant h_- is the coefficient of negative taxis of P on the gradient of Z (prey-evading predators), and h_+ is the coefficient of positive taxis of Z on the gradient of P (predators pursuing prey). For simplicity, the diffusion coefficient D is considered constant, uniform, and equal for both species. In this paper we consider problems in one spatial dimension, $\mathbf{r}=(x)$, and in two spatial dimensions, $\mathbf{r}=(x, y)$.

We consider the local kinetics functions $f(P, Z)$ and $g(P, Z)$, describing the population dynamics of prey (phytoplankton) P and predators (zooplankton) Z , in the Holling type-III form used by Truscott and Brindley [5]. In nondimensional form these are

$$f(P, Z) = \beta P(1 - P) - ZP^2/(P^2 + \nu^2),$$

$$g(P, Z) = \gamma ZP^2/(P^2 + \nu^2) - wZ. \quad (2)$$

It is known that at an appropriate choice of parameters, these kinetics demonstrate “excitable” behavior, and the reaction-diffusion system (1) with $h_- = h_+ = 0$ has propagating solitary wave solutions [5,6].

We have studied properties of population taxis waves in the mathematical model (1) and (2) for one-dimensional (1D) [1,2] and two-dimensional (2D) [3] cases. In those works, we have shown that inclusion of the taxis terms can radically change the properties of propagating waves, compared to the much better studied waves in purely reaction-diffusion systems without taxis. We have demonstrated that the very mechanism of propagation of waves in such systems is different. Here are some peculiar features of taxis waves, described in Refs. [1,2].

(a) Essentially different shape of the wave profiles. For the $P(x-ct)$ profile, it could be either a “single-hump” or “double-hump” shape.

(b) The dependence of the wave-propagating velocity on the taxis coefficients has two distinct branches, “parabolic” and “linear.” The transition from one branch to the other correlates with changes in the shape of the wave profiles: the parabolic branch of this graph corresponds to a double-hump shape of the $P(x-ct)$ profile, and the linear branch corresponds to a single-hump shape.

(c) In the space of parameters of Eq. (1), there are large regions, where waves demonstrate quasisoliton interaction: they can penetrate through each other, and also reflect from impermeable boundaries, see Fig. 1(a)–1(c).

(d) For some regions in the parameter space, taxis waves can spontaneously split, emitting “backward”- propagating waves. This can be observed both in the case of solitonlike interaction [Fig. 1(a), solid triangles] and in the case of annihilating waves [Fig. 1(a), hollow triangles]. The backward-

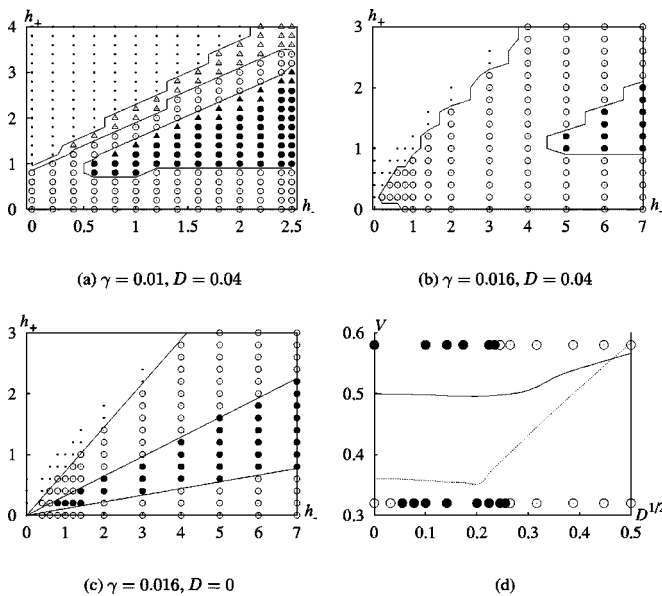


FIG. 1. (a),(b),(c) Parametric regions corresponding to different regimes of taxis waves ($\beta=1, w=0.004$). Solid circles: quasisoliton waves. Solid triangles: quasisolitons with the wave splitting. Hollow circles: stably propagating waves annihilating on collision. Hollow triangles: splitting waves annihilating on collision. Dots: no propagating wave solution. (d) Wave-propagation velocity as a function of the square root of the diffusion coefficient. Solid line and the upper row of symbols: $\gamma=0.016, h_-=5, h_+=1$. Dotted line and the lower row: $\gamma=0.01, h_-=h_+=1$. In reaction-diffusion systems, this dependence is always a straight line. Here and on other figures, all parameters and variables are dimensionless.

emitted waves with time either decay, or split themselves. In the latter case, the chain of splitting events can lead to self-supporting, aperiodic, or approximately periodic activity.

(e) The dependence of the propagation velocity on diffusion in this system differs from the square-root dependence, always valid for reaction-diffusion waves, see Fig. 1(d).

Additionally, in two spatial dimensions, we observed the following [3]:

(f) Partial reflection of waves from boundaries, or their partial penetration through each other.

(g) ‘‘Swollen tips,’’ i.e., circular wave sources, produced by free ends of broken waves.

(h) Attachment of free ends of broken waves to the wave backs.

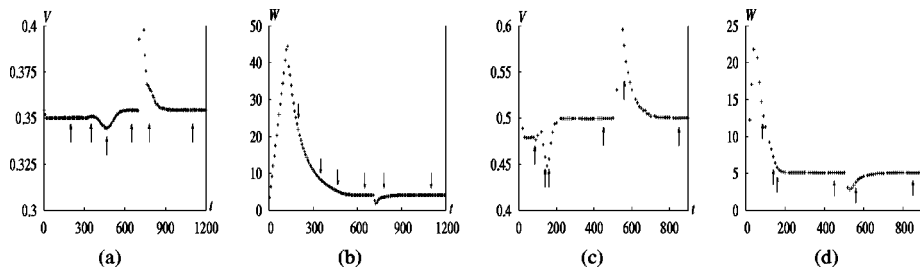


FIG. 3. Variations of the propagation velocity (a),(c) and wave width (b),(d) during the transient, corresponding to Fig. 2: (a),(b) $\gamma=0.01, D=0.04, h_-=h_+=1$, (c),(d) $\gamma=0.016, D=0, h_-=5, h_+=1$. Width $W(t)$ is defined as the distance between the points on the front and the back of the wave where $P(x,t)=0.4$; propagation velocity $V(x,t)$ is defined as the instant velocity of such a point on the front, i.e., where $P(x,t)=0.4$ and $\partial P/\partial t(x,t) > 0$. Arrows designate the time moments, for which Figs. 4 and 5 show the wave profiles.

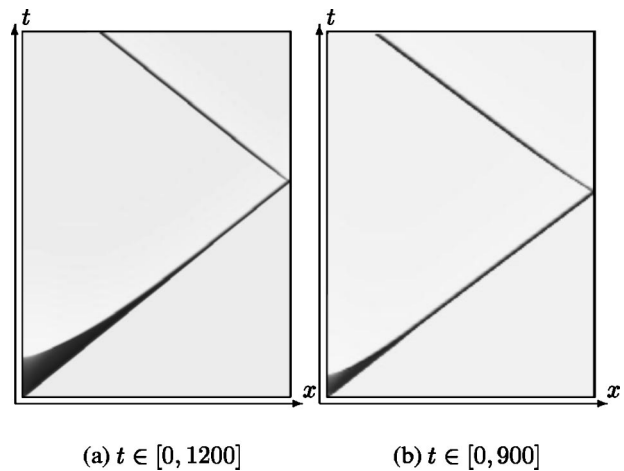


FIG. 2. The spatiotemporal dynamics of the taxis wave formation, propagation, and reflection from impermeable boundaries for system (1) in one-dimensional case with $L=250$: (a) $\gamma=0.01, D=0.04, h_-=h_+=1$; (b) $\gamma=0.016, D=0, h_-=5, h_+=1$. Black corresponds to $P=0.9$, white to $P=0$.

In this paper, by numerical simulation of systems (1) and (2) we demonstrate a type of wave interaction, in which of two colliding waves, one annihilates and the other continues to propagate. For brevity, we call this behavior ‘‘half-soliton.’’

II. DETAILS OF THE MODEL AND NUMERICAL METHODS

We used ‘‘upwind’’ schemes to approximate the taxis terms $\mathcal{L}u = (\partial/\partial x)u(x,t)[\partial S(x,t)]/\partial x$. The idea of the upwind schemes is that they use not the mean between values of the variables subject to taxis at two neighboring grid nodes as in the central scheme, but select one or the other depending on the direction of taxis, i.e., the sign of the gradient of the attractant. For details of the schemes we used, see our previous work [2]. As we have shown in Ref. [2], the implicit central scheme only works for Eq. (1) if $D > 0$, whereas our upwind schemes work for $D=0$ as well. We used a time-implicit scheme with discretization steps $\delta x=0.1$, and $\delta t=5 \times 10^{-3}$ for one-dimensional simulations, and a time-explicit one with discretization steps for $\delta x=\delta y=0.5$ and $\delta t=5 \times 10^{-3}$ for two-dimensional calculations.

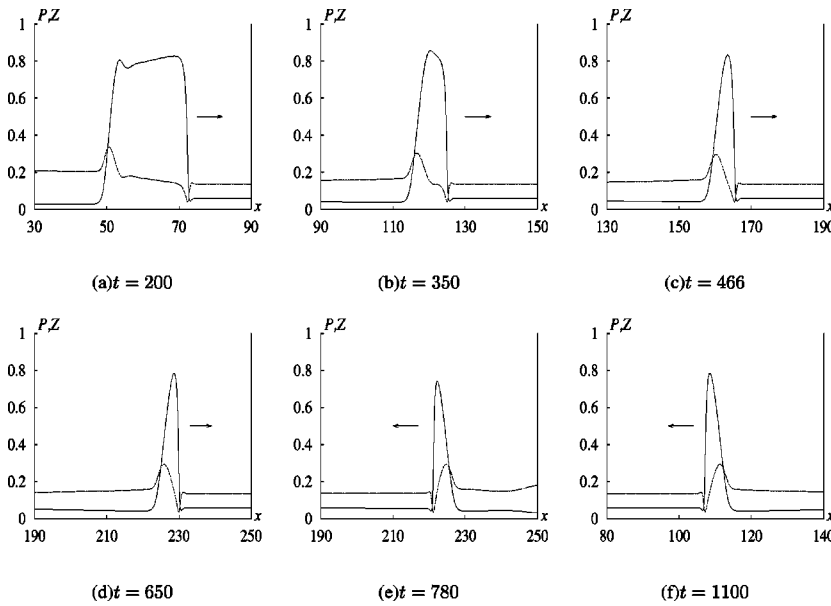


FIG. 4. Variations of the wave profiles, corresponding to the selected time moments in Figs. 2(a), 3(a), and 3(b).

Unless specified otherwise, we have used the same parameters in Eq. (1) in our numerics, as we used in Ref. [2], that is $\beta=1$, $\nu=0.07$, $w=0.004$, and two different values of γ : $\gamma=0.01$, henceforth “small γ ,” which allows propagation of purely reaction-diffusion waves, i.e., with $h_+=h_-=0$, $D>0$; and $\gamma=0.016$, henceforth “large γ ,” for which purely reaction-diffusion waves do not propagate, and taxis is required [see Fig. 1(a)–1(c)]. Systems (1) and (2) are nondimensionalized, thus all the variables and parameters are dimensionless.

In all numerics, we used nonflux boundary conditions: $\partial P/\partial x|_{x=0,L}=0$ and $\partial Z/\partial x|_{x=0,L}=0$ for one-dimensional problems, $x \in [0, L]$, and $\partial P/\partial x|_{x=0,L_x}=0$, $\partial Z/\partial x|_{x=0,L_x}=0$, and $\partial P/\partial y|_{y=0,L_y}=0$, $\partial Z/\partial y|_{y=0,L_y}=0$ for two-dimensional problems, $(x, y) \in [0, L_x] \times [0, L_y]$.

III. “HALF-SOLITON” WAVE INTERACTION IN ONE-DIMENSIONAL CASE

Figure 2 illustrates spatiotemporal dynamics of population taxis waves in Eq. (1), including their formation, propagation, and reflection from boundaries. The waves were initiated, both for small γ , panel (a), and for large γ , panel (b), by setting initial conditions for $P(x, 0)=0.8$ for $x \in [0, 1]$ and $P(x, 0)$ for $x \in (1, L]$ and $Z(x, 0)$ for $x \in [0, L]$ equal to their equilibrium values.

The key observation for the present paper is that taxis waves establish their stationary structure and corresponding speed only after a rather long transient. Figure 3 illustrates variations of the propagation velocity, V [panels (a) and (c)] and width, W [panels (b) and (d)] of a wave during such transients, both before and after its reflection from the

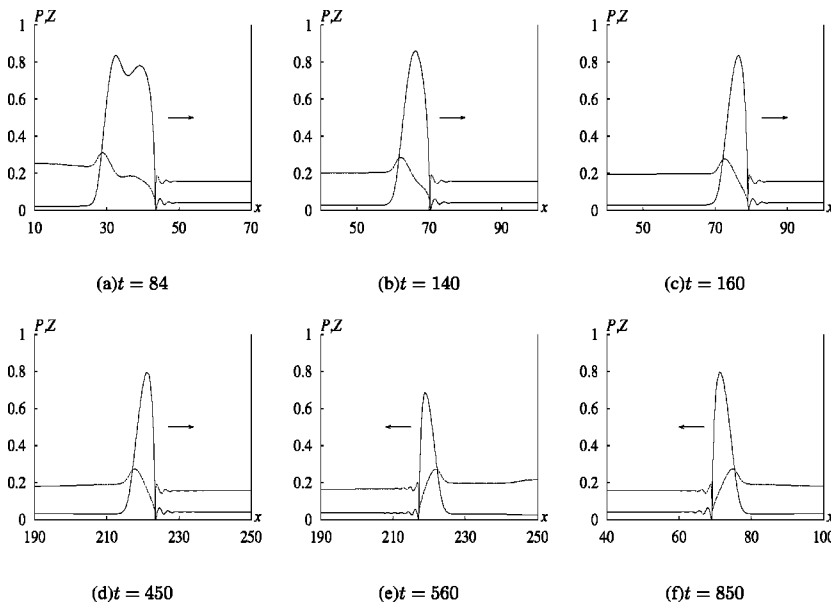


FIG. 5. Variations of the wave profiles, corresponding to the selected time moments in Figs. 2(b), 3(c), and 3(d).

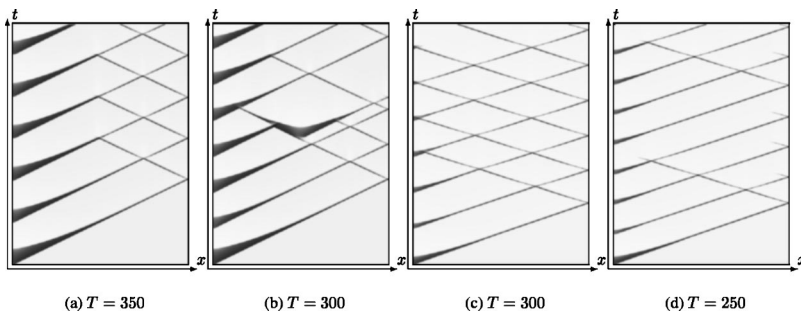


FIG. 6. The spatiotemporal dynamics of the taxis waves periodically initiated at the left end, with time period T , specified under the density plots. Independent variables ranges: $L=250$, $t \in [0, 2000]$. (a) and (b): $\gamma=0.01$, $D=0.04$, $h_- = h_+ = 1$; (c) and (d): $\gamma=0.016$, $D=0$, $h_- = 5$, $h_+ = 1$.

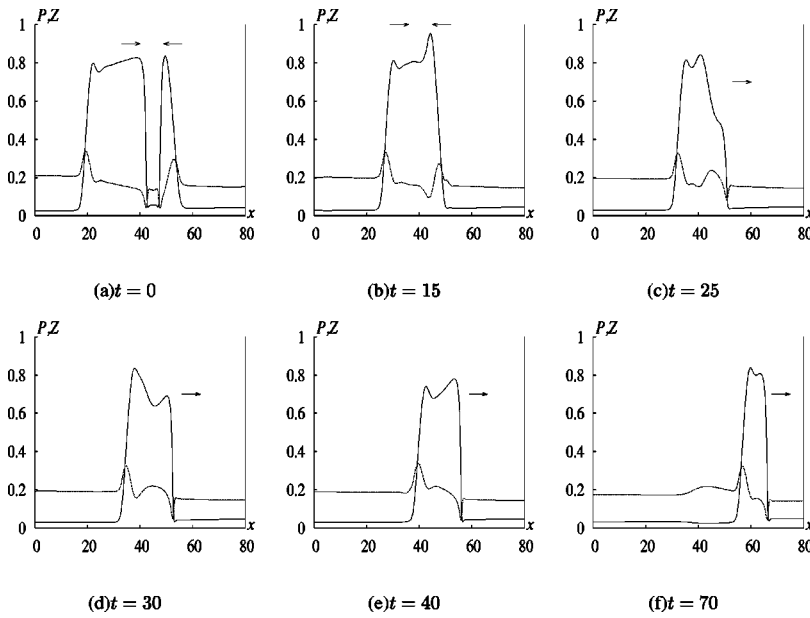


FIG. 7. Collision of W_{200} (from the left) and W_{466} (from the right). Parameters $\gamma=0.01$, $D=0.04$, $h_- = h_+ = 1$.

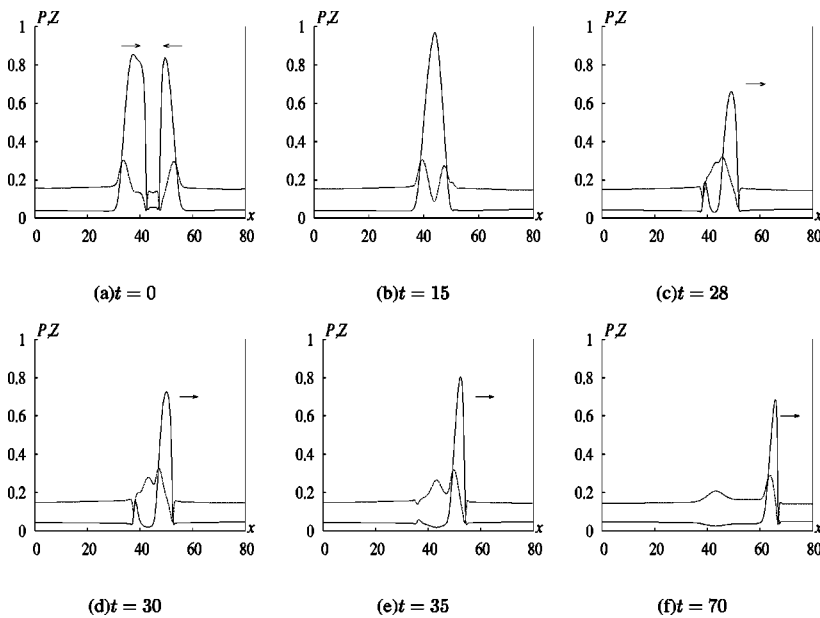


FIG. 8. Collision of W_{350} (from the left) and W_{466} (from the right). Parameters $\gamma=0.01$, $D=0.04$, $h_- = h_+ = 1$.

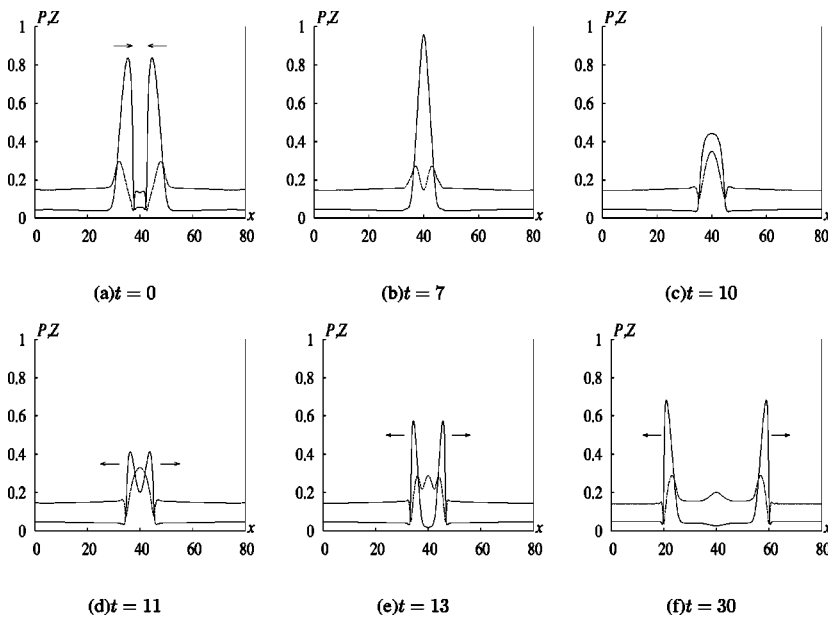


FIG. 9. Collision of W_{466} (from the left) and W_{466} (from the right). Parameters $\gamma=0.01$, $D=0.04$, $h_- = h_+ = 1$.

boundary. During the transient, the propagation velocity distinctly decreases for a short interval of time (approximately between $t=450$ and 550), while the wave width continues to monotonically approach its stationary value. This temporary decrease of the velocity correlates with a change in the shape of the wave profile. Figures 4 and 5 show the wave profiles corresponding to selected time moments, indicated by arrows on Fig. 3. We see that the temporary decrease of propagation velocity corresponds to the transition of the wave profile from a double-hump to a single-hump shape. As mentioned earlier, in Ref. [2] we have shown that these two shapes correspond to two distinct branches on the graph of stationary propagation speed V on h_+ , “parabolic” and “linear.” Figures 4 and 5 demonstrate that the transition from one shape to the other happens during the transient, and thus associated variations in the propagation velocity seen in Fig. 3. Besides, the change of shape itself causes apparent short-term change

in the velocity due to the method of measuring the velocity of the wave, as the velocity of the point with a particular value of P ; this is the main reason with the sharp local minima of the propagation velocity coinciding with the transitions from one wave shape to the other.

On the other hand, the type of interaction of stationary waves, i.e., reflection or annihilation (see Fig. 1), also correlates with the shape of the profiles of those waves [2]. Since the shape of the profiles changes in the long transient after the wave initiation, we decided to check if the waves at different stages of their “lives” will show different types of interaction, corresponding to their current shape. This conjecture has been tested by numerical experiments, the results of which are presented in Fig. 6. Periodic waves were initiated in a one-dimensional medium with nonflux boundaries. In addition to already-known quasisoliton reflection of waves and their splitting, we have observed also a type of interac-

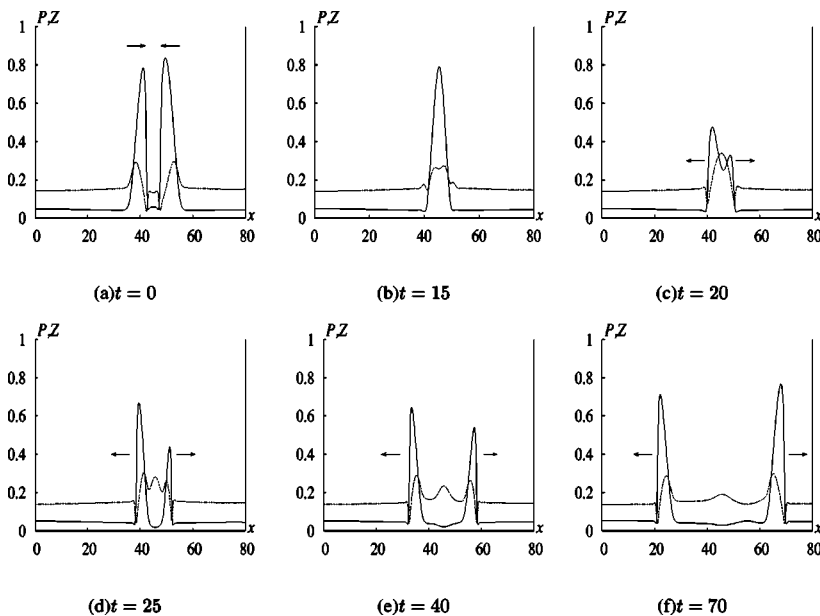


FIG. 10. Collision of W_{650} (from the left) and W_{466} (from the right). Parameters $\gamma=0.01$, $D=0.04$, $h_- = h_+ = 1$.

TABLE I. Results of collisions for $\gamma=0.01$, $D=0.04$, $h_-=h_+=1$. Here “A” denotes W_{200} , “B” is W_{350} , “C” is W_{466} , “D” is W_{650} . The result of the collision is shown on the intersection of the corresponding row and column, the letter denotes the surviving wave, “+” means both waves survive, “-” means neither survives. Approximate ratios of widths ($P=0.4$) are: $\lambda_A/\lambda_D=5.3$, $\lambda_B/\lambda_D=2$, $\lambda_C/\lambda_D=1.25$.

	A	B	C	D
A	-	A	A	A
B	A	+	B	B
C	A	B	+	+
D	A	B	+	+

tion where of two colliding waves, only one survives, whereas the other decays. We call this “half-soliton” interaction.

For a detailed study of this half-soliton interaction, we simulated collisions of artificially prepared taxis waves of different “ages.” We have recorded a wave in a large medium at chosen moments of its transient, namely, $t=195, 345, 461$, and 645 ; (all by five time units earlier than the moments shown on Fig. 4). Then we set up initial conditions, in which in one-half of the medium we used a recorded wave of one age, suitably shifted along the x axis, and in the other half of the medium we used another recorded wave. Of course, the wave in the right half of the medium was also inverted, so as to move towards the left wave. As the time from such artificial initial conditions to the collision was approximately five time units, the ages of waves at the very moment of collision correspond to those shown in Fig. 4. So, we denote such waves as $W_{200}, W_{350}, W_{466}$, and W_{650} , according to their ages.

Figure 7 describes interaction of waves W_{200} and W_{466} . The result is that W_{200} has suppressed W_{466} . Similar events are shown in Figs. 8 (W_{350} vs W_{466}), 9 (W_{466} vs W_{466}), and 10 (W_{650} vs W_{466}). Tables I and II summarize the results of collisions of waves of various ages.

These results suggest that the half-soliton interaction takes place when the two colliding waves are essentially different in their widths. A thinner, older wave is less likely to penetrate through a younger, thicker wave. Note that since the colliding waves now are different from each other, we

TABLE II. Results of collisions for $\gamma=0.016$, $D=0$, $h_-=5$, $h_+=1$. Here “a” is w_{84} , “b” is w_{140} , “c” is w_{160} , “d” is w_{450} , corresponding to the selected moments indicated on Fig. 2, see also Figs. 3(c) and 3(d). The approximate ratios of widths ($P=0.4$) are: $\lambda_a/\lambda_d=2.8$, $\lambda_b/\lambda_d=1.4$, $\lambda_c/\lambda_d=1.14$.

	a	b	c	d
a	-	a	a	a
b	a	-	b	b
c	a	b	+	+
d	a	b	+	+

can distinguish “reflection” from “penetration” of the waves, and the most natural interpretation is that the waves penetrate through each other, if they do, rather than reflect.

IV. HALF-SOLITONS IN TWO DIMENSIONS

In our previous work [3], we have described some typical two-dimensional regimes of propagation of taxis waves in Eqs. (1) and (2). In particular, we have demonstrated that for parameters corresponding to quasisoliton behavior in one dimension, concentric waves can either penetrate/reflect on collision, or annihilate, depending on conditions, particularly on the curvature of the waves. The results of the previous section show, however, that another factor that can affect the result of collision, is the “age” state of the colliding waves.

Let us consider the interaction of concentric taxis waves of different radii and different widths. As in one-dimensional collisions, the initial conditions have been prepared from solitary one-dimensional pulses recorded at different stages of their transients and therefore having different widths. If $P_{1d}(x), Z_{1d}(x)$ is such a recording, shifted along the x axis so that the front is at $x=0$, then initial conditions we used can be described as

$$P(x,y,0) = P_{1d}(\sqrt{x^2 + y^2} - R), \quad Z(x,y,0) = Z_{1d}(\sqrt{x^2 + y^2} - R),$$

where R was the desired radius of the circular wave.

For parameters $\gamma=0.016, D=0, h_-=5, h_+=1$, we initiated a one-dimensional wave in the standard way described above, and recorded it at times $t=120$ (as wave W), $t=150$

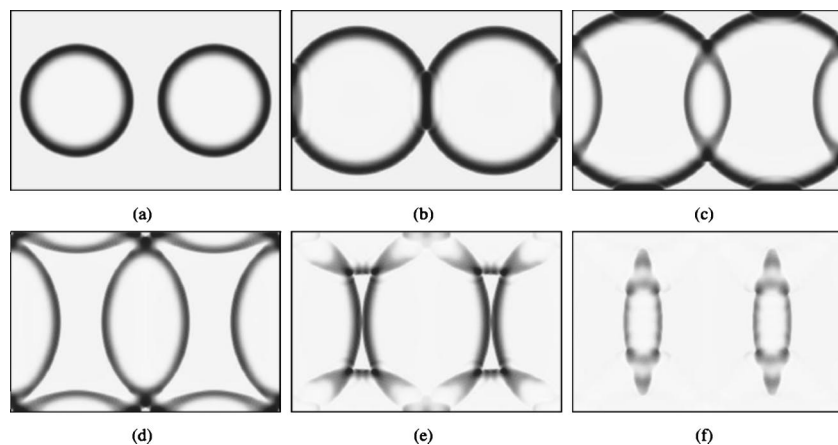


FIG. 11. Quasisoliton interaction of two U waves with initial radii $R=70$. Time interval between the panels is 20. Medium size $L_x \times L_y = 150 \times 100$.

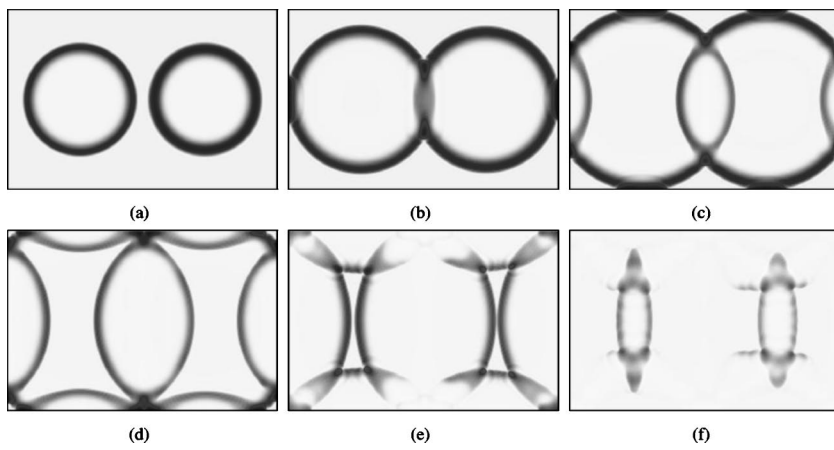


FIG. 12. Quasisoliton interaction of a *U* wave and an *S* wave with initial radii $R=70$. Time interval between the panels is 20. Domain size $L_x \times L_y = 150 \times 100$.

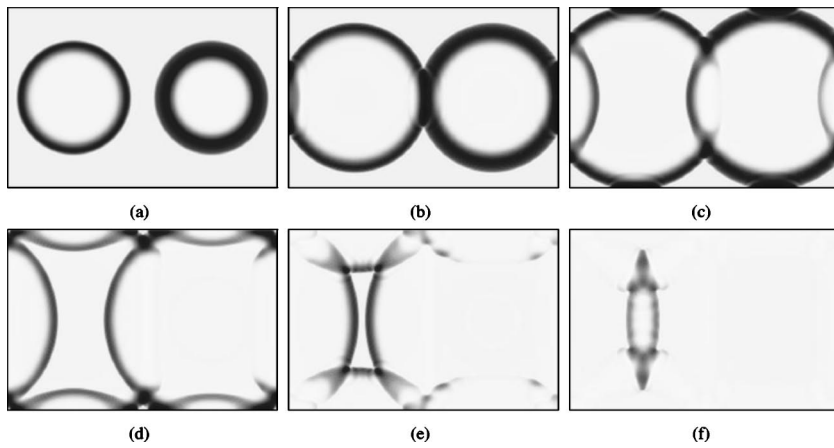


FIG. 13. Half-soliton interaction of a *U* wave and a *W* wave with initial radii $R=70$. Time interval between the panels is 20. Domain size $L_x \times L_y = 150 \times 100$.

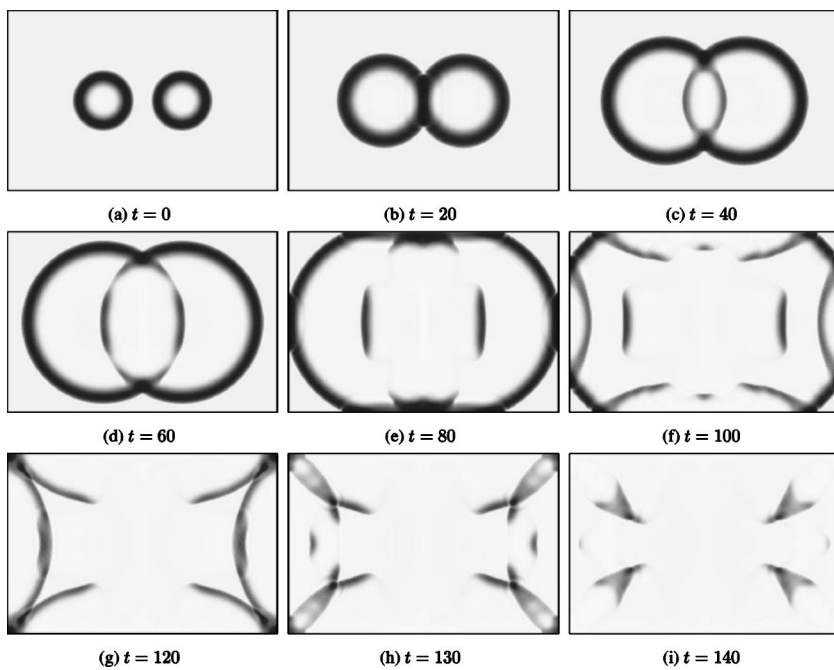


FIG. 14. Interaction of two *S* waves with initial radius $R=40$. Timing is shown under the panels. Domain size $L_x \times L_y = 150 \times 100$.

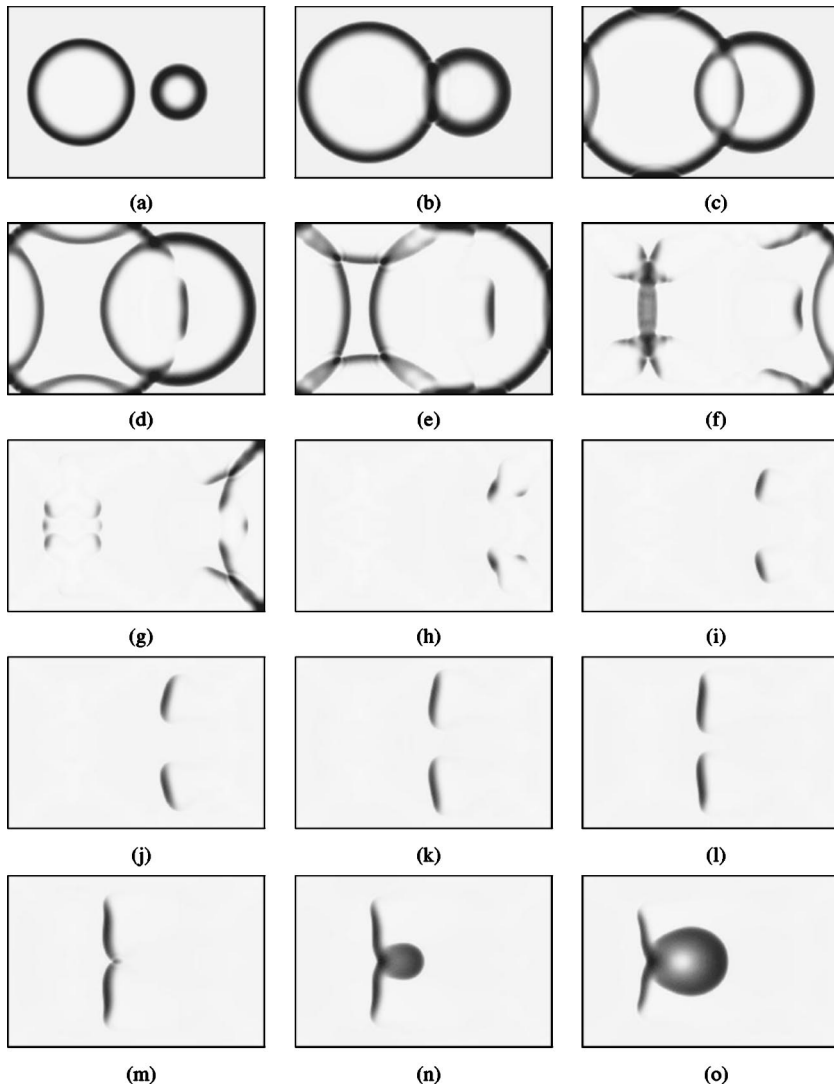


FIG. 15. The interaction of a U wave with initial radius $R=70$ and an S wave with initiation radius $R=40$. Time interval between the panels is 20. Domain size $L_x \times L_y = 150 \times 100$.

(wave S), and $t=450$ (wave U). These recorded waves had widths, measured at level $P=0.4$, correspondingly, $\lambda_W=9.2$, $\lambda_S=6.4$, and $\lambda_U=5.1$, so that $\lambda_W/\lambda_U=1.8$ and $\lambda_S/\lambda_U=1.25$.

Figure 11 shows the interaction of two U waves with initial radius $R=70$. In this case, the waves both penetrate through each other and reflect from the domain boundaries. Similar quasisoliton interaction is observed on collision of a U and an S waves with equal radii $R=70$, see Fig. 12. The interaction of U and W waves with the same radii demonstrates a half-soliton behavior, when wave W suppresses U , but annihilates at the boundary, see Fig. 13 .

The collision of two S waves with initial radii $R=40$, see Fig. 14, produces spatially localized waves, which we call “taxitons” [panels (d)–(f)]. These taxitons interact in a half-soliton way with waves reflected from the boundaries [panels (g), (h)].

There are also simulations showing both half-soliton and taxiton regimes at the same time. In Fig. 15, wave U with initial radius $R=70$ collided with wave S with initial radius $R=40$. The result was that the S wave penetrated through U in the half-soliton way, and the U wave penetrated only partially, as a taxiton [panels (c)–(e)]. This is followed by an even more complicated picture of different kinds of interactions, including tip swelling as described in Ref. [3] [panels (n), (o)].

The type of interaction (annihilation, quasisoliton, or half-soliton) depends not only on the curvature and width of the colliding waves, but also on the angle of collision. This explains the formation of the taxitons, where only a part of a wave continues to propagate after collision, even though all parts of the wave are of the same age. The waves colliding head on are more likely to penetrate than in a skewed colli-



FIG. 16. The interaction of two plane U waves, with an initial angle of 80° between them. Time interval between the panels is 20. Domain size $L_x \times L_y = 150 \times 50$.



FIG. 17. The interaction of two plane U waves, with an initial angle of 60° between them. Time interval between the panels is 30. Domain size $L_x \times L_y = 150 \times 50$.

sion, and so when the widths of the waves are close to their critical values allowing penetration, only the part of the wave that is close to first collision site penetrates, whereas more distant parts annihilate.

Figures 16 and 17 illustrate collision at different angles in pure form. Initial conditions have been formed from the same 1D wave U (old age, well established), arranged in two dimensions in the form of two plane waves meeting each other at different angles, i.e.,

$$P(x, y, 0) = P_{1d}[x \cos(\theta) + y \sin(\theta) - C],$$

$$Z(x, y, 0) = Z_{1d}[x \cos(\theta) + y \sin(\theta) - C],$$

where θ and C are constants, different for the left and the right halves of the medium.

In Fig. 16, the angle between the fronts of the waves is 80° , and the waves annihilate. In Fig. 17, the angle is 60° , and the waves penetrate through each other. This proves directly that result of collision depends on the angle of incidence.

V. CONCLUSIONS

In our previous papers [1–3] we have described soliton-like behavior and also spontaneous wave splitting in a class of waves that can exist in population dynamics models due to taxis of species to each other’s gradients. It was shown that properties of taxis waves are essentially different from those of solitary waves observed in excitable reaction-diffusion systems.

In the present paper we have described properties of such taxis waves.

(a) “Half-soliton interaction,” when only one of the colliding waves penetrates and the other annihilates. This is observed both in one and in two spatial dimensions.

(b) “Taxitons,” i.e., compact pieces of solitary waves in two dimensions, that can form when only a part of a colliding wave can manage to penetrate through the collision.

We have demonstrated that half-soliton interaction depends on the width of the colliding waves, which can depend on their history, and formation of taxitons depends on that too, and also on the angle of incidence between the colliding waves. The dependence on the angle of incidence is apparently related to the dependence on the wave width, as in an oblique collision, the apparent width of the waves along the line of collision is larger.

So, the results of the present and previous works [1–3] demonstrate that population taxis waves have unique properties, making them different both from solitons in conservative systems [7], and from solitary waves in excitable reaction-diffusion systems [8,9]. A broader investigation of this new class of nonlinear waves is required, which is both interesting from mathematical viewpoint, and also motivated by recent experimental studies of chemotaxis in bacteria [10,11], which demonstrated interesting results on propagation and interaction of population taxis waves, and also on the self-organization of population systems with taxis [12–22].

ACKNOWLEDGMENTS

This study was supported in part by EPSRC Grant No. GR/S08664/01 (U.K.) and RFBR Grant No. 03-01-00673 (Russia).

[1] M. A. Tsyganov, J. Brindley, A. V. Holden, and V. N. Biktashev, *Phys. Rev. Lett.* **91**, 218102 (2003).
 [2] M. A. Tsyganov, J. Brindley, A. V. Holden, and V. N. Biktashev, *Physica D* (to be published), e-print nlin.PS/0406013.
 [3] V. N. Biktashev, J. Brindley, A. V. Holden, and M. A. Tsyganov, *Chaos* (to be published), e-print nlin.PS/0406012.
 [4] E. F. Keller and L. A. Segel, *J. Theor. Biol.* **30**, 225 (1971).
 [5] J. E. Truscott and J. Brindley, *Philos. Trans. R. Soc. London, Ser. A* **347**, 703 (1994).
 [6] L. Matthews and J. Brindley, *Dyn. Stab. Syst.* **12**, 39 (1997).
 [7] R. K. Dodd, J. Eilbeck, J. Gibbon, and H. Morris, *Solitons and Nonlinear Waves Equations* (Academic, London, 1984).
 [8] A. von Oertzen, A. S. Mikhailov, H. H. Rotermund, and G. Ertl, *J. Phys. Chem. B* **102**, 4966 (1998).
 [9] O. V. Aslanidi and O. A. Mornev, *J. Biol. Phys.* **25**, 149 (1999).
 [10] J. Adler, *Science* **153**, 708 (1966).
 [11] J. Adler, *J. Bacteriol.* **92**, 121 (1966).
 [12] G. R. Ivanitskii, A. B. Medvinskii, and M. A. Tsyganov, *Usp. Fiz. Nauk* **161**, 13 (1991).
 [13] G. R. Ivanitskii, A. B. Medvinskii, and M. A. Tsyganov, *Usp. Fiz. Nauk* **164**, 1041 (1994).
 [14] K. Agladze, E. Budrene, G. Ivanitsky, V. Krinsky, V. Shakhbazyan, and M. Tsyganov, *Proc. R. Soc. London, Ser. B* **253**, 131 (1993).
 [15] M. A. Tsyganov, I. B. Kreteva, A. B. Medvinskii, and G. R. Ivanitskii, *Dokl. Akad. Nauk* **333**, 532 (1993).
 [16] M. A. Tsyganov, I. B. Kreteva, G. V. Aslanidi, K. B. Aslanidi, A. A. Deev, and G. R. Ivanitsky, *J. Biol. Phys.* **25**, 165 (1999).
 [17] T. Hofer, J. A. Sherratt, and P. K. Maini, *Physica D* **85D**,

- 425 (1995).
- [18] B. N. Vasiev, P. Hogeweg, and A. V. Panfilov, *Phys. Rev. Lett.* **73**, 3173 (1994).
- [19] E. O. Budrene and H. Berg, *Nature (London)* **349**, 630 (1991).
- [20] E. O. Budrene and H. Berg, *Nature (London)* **376**, 49 (1995).
- [21] E. Ben-Jacob, O. Schochet, A. Tenenbaum, I. Cohen, A. Czirok, and T. Viscek, *Nature (London)* **368**, 46 (1994).
- [22] M. Mimura, H. Sakaguchi, and M. Matsushita, *Physica A* **282**, 283 (2000).